iJRASET
International Journal For Research in Applied Science and Engineering Technology

INTERNATIONAL JOURNAL FOR RESEARCH

IN APPLIED SCIENCE & ENGINEERING TECHNOLOGY

Volume: 7 **Issue:** I **Month of publication:** January 2019

DOI: http://doi.org/10.22214/ijraset.2019.1022

www.ijraset.com

Call: 08813907089 | E-mail ID: ijraset@gmail.com

International Journal for Research in Applied Science & Engineering Technology (IJRASET)
ISSN: 2321-9653; IC Value: 45.98; SJ Impact Factor: 6.887
Volume 7 Issue I, Jan 2019- Available at www.ijraset.com

Ethyl(S)-(−)-4-chloro-3-hydroxybutyrateStudy by D.F.T

Piyush Gupta[1], Rahul Tripathi[2], C. K Dixit[3], Sanjeev Kumar Trivedi[4]
[1]*North East Frontier Technical University, Arunachal Pradesh-791001*
[2, 3]*Mumtaz P.G College, Lucknow University, Lucknow-226020*
[4]*D.S.M.N.R University, Lucknow -226017*

Abstract: ***Active chirals like 4-chloro-3-hydroxybutanoicS acids and esters are very important as chiral building blocks in pharmaceutical industries. Its enantiomers are precusors, being important to starting materials like enzyme inhibitors .The asymmetric reduction of ethyl 4-chloro-3-oxobutanoate using glucose, glycerol, or 2-propanol as a co-substrate in production of (S)- and (R)- 4-chloro- 3-hydroxybutyrate was achieved by Hunt et.al. [Hunt, 1995]. Many studies have been reported on the microbial or enzymatic asymmetric reduction of similar acids and esters. Optically active 4-chloro-3- hydroxybutyrate, which is a chiral chloroalcohol having a C_4 structural skeleton, are employed in the synthesis of biologically and pharmacologically important compounds like (R)-carnitine, (R)-4-hydroxy-2-pyrrolidone. These are a physiologically significant agent, involved in the metabolism of long-chain fatty acids through the mitochondrial membrane in the human body. One such important molecule is Ethyl (S)-(–)-4-chloro-3- hydroxybutyrate. Though hazardous to eyes and skin, it is useful as chiral building blocks for the synthesis of chiral pharmaceuticals, insect pheromones and others. The 4- chloro-3-hydroxybutyrate is synthesized from natural products like L-malic acid, dimethyl L-malic acid, l-ascorbic acid or l-asparatic acid [Suzuki, 1999], and synthesized further by microbial reduction with subsequent substitutions.***

Keywords: Density Functional Theory, IR, Raman, Electronic Parameter, Thermodynamic parameter, Molecular Orbital, MESP.

I. INTRODUCTION

We present conformational and vibrational analysis of Ethyl (S)-(–)-4-chloro-3-hydroxybutyrate ($C_6H_{11}O_3Cl$). A broad IR band near 3450 cm^{-1} is presumably due to the bonded O-H stretch. The C=O stretching mode is observed near 1729 cm^{-1}. The shift of these bands though not much (about 4% and 2% respectively) indicates that both the groups are involved in forming a dimer of the type O-H•••O=C hydrogen bond. Another IR band due to C=O stretch is observed at 1630 cm^{-1}. The proposed dimer model consists of four dimers arising from the combination of monomer conformers but unlike the one proposed for (R)-(+)-Methylsuccinic acid there is a lack of local centre of inversion and hence the mutual exclusion rule is not satisfied because two IR bands are attributed to C=O vibration[1]. It will be shown that the most stable dimer has a population of ~90% while the remaining four have 10%. We do not rule out the existence of monomers as independent species completely as most of the dimer and monomer frequencies are nearer to each other.

A. Results and Discussion

1) Monomer and Dimer Analysis

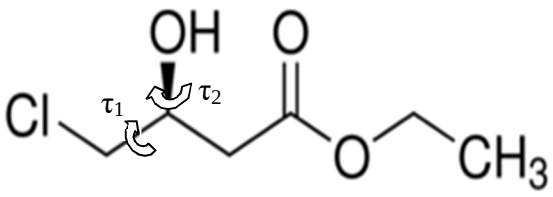

Fig1.1: Molecular structure of Ethyl (S)-(–)-4-chloro-3-hydroxybutyrate

The molecular structure of Ethyl (S)-(−)-4-chloro-3-hydroxybutyrate is shown in Fig.

a) The experimental IR and Raman spectra, as shown in Fig1.2, are characterized by band features not amenable to straight forward spectral interpretation.

The IR region 3500 – 2500 cm^{-1} is dominated by broad structureless absorption with identifiable peaks at 3452 and 2982 cm^{-1}. Further, there is an intense and rather broad absorption band near 1730 cm^{-1}. . Other absorption bands are somewhat sharp but covered in broad envelope with one isolated broad band near 1400-900 cm^{-1}. The characteristic CH, CH_2, CH_3 and CC bands are all identified in absorption spectrum and correlated in the Raman spectrum. The bands are diffused and lumpy in nature because of the *inter*- molecular influences.[2] In all the previous chapters where we have identified such similar characters in the vibration spectra in molecules like (R)-(–)-2-Pyrrolidinemethanol, (R)-(+)- Methylsuccinic acid, we have accounted for a DFT hydrogen bonded dimer model satisfactorily explaining the features. The down-shifted bands near 3430 and 1730 cm^{-1} are evidences in itself that the O-H and C=O are participating into forming a hydrogen bond of the type O-H•••O=C bond. In molecules (R)-(+)-Methylsuccinic acid and (S)-2- Bromo-3-chloropropionic acid, we have seen the bands due to C=O stretching, appearing mutually exclusive in IR and Raman as asymmetric and symmetric modes near 1700 and 1650 cm^{-1}. But unlike in the molecules (S)-2-Bromo-3-phenylpropionic acid and (R)-(+)- Methylsuccinic acid as discussed in Chapter 5 and 6 respectively, here we have a Raman mode at the same position as IR near 1730 cm^{-1}, which rules out the idea that the molecule may form a centre of inversion upon hydrogen bonding. Investigation of the basis of these aspects we propose both monomer and dimer model to explain the observed spectra.

To investigate the structure of monomers we performed a relaxed potential energy surface scan (PES) at RHF/3-21G level of theory to confirm the orientation of O- H and C-Cl with respect to the skeleton of the molecule, we simultaneously varied the dihedral angle C5-C2*-C1-Cl16 (τ_1) and C5-C2*-O17-H18 (τ_2) (where C* refers to the carbon atom at chiral centre in the molecule $C_6H_{11}O_3Cl$).

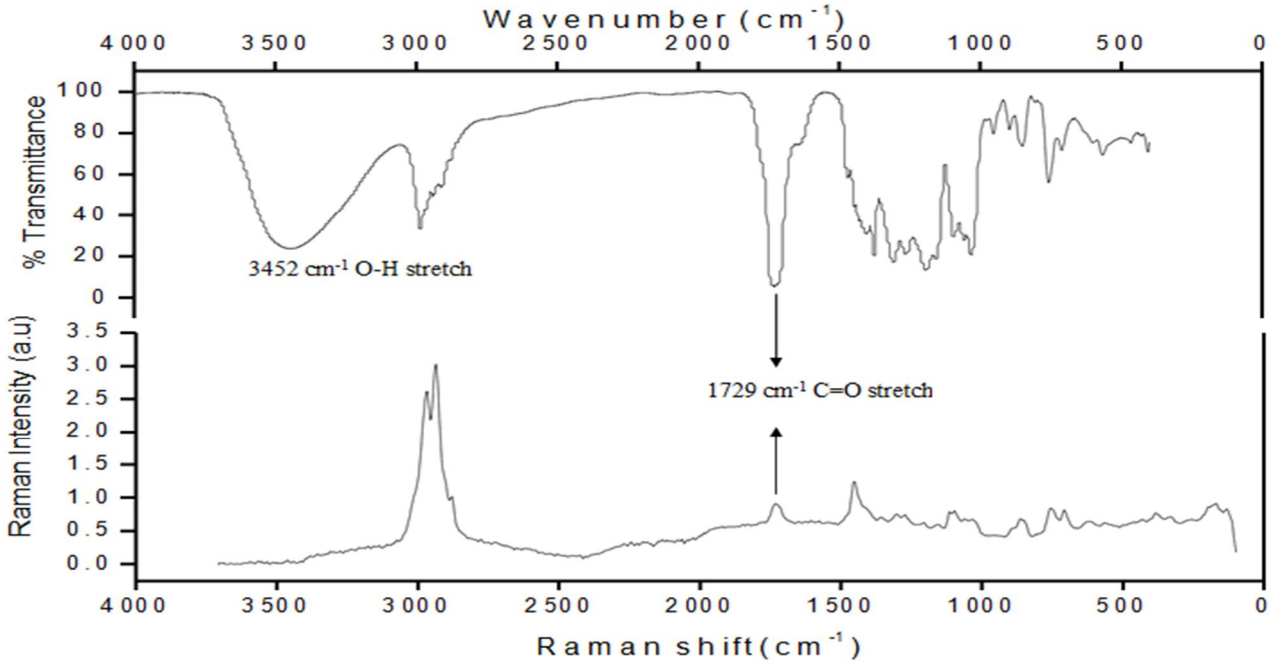

Fig. 1.2: Experimental IR and Raman spectra of Ethyl (S)-(–)-4-chloro-3-hydroxybutyrate

We found three conformers on the PES curves as shown in Fig. 1.3. We further optimized the structures of the three conformers by performing harmonic frequency analysis at B3LYP/6-311+G(d,p) level by taking the PES results at RHF/3-21G level as input. The calculations yielded three conformers called $\boldsymbol{C_1}$, $\boldsymbol{C_2}$, and $\boldsymbol{C_3}$ that are shown in Fig. 1.4 (a), (b) and (c). The $\boldsymbol{C_1}$ is the most stable conformer with a population of 82.8%; the second most stable conformer is $\boldsymbol{C_2}$ with a population of 9.6%, being separated from $\boldsymbol{C_1}$ by 1.281 kcal/mol. The least populated conformer $\boldsymbol{C_3}$ with ~7% is separated from $\boldsymbol{C_1}$ by 1.427 kcal/mol. The Relative Gibbs energies and populations computed at B3LYP/6- 31+G(d,p) level are given in Table 1.1. In Table 1.2 we present the optimized geometrical parameters of all the three conformers $\boldsymbol{C_1}$, $\boldsymbol{C_2}$, and $\boldsymbol{C_3}$.

From the conformers structures we see that the hydroxyl O-H is always oriented close to the carbonyl 'O'. A possibility that the attraction here could be *intra*-molecular type cannot be ruled out. Thus we tried to model the hydrogen bonding considering the O-H•••O=C type with-in the hydroxyl and carbonyl monomers of the same monomer. The energies for this modeling are the same as the ones presented in Table 1.1 for all the three conformers, and hence the frequencies are also reproduced.

ISSN: 2321-9653; IC Value: 45.98; SJ Impact Factor: 6.887
Volume 7 Issue I, Jan 2019- Available at www.ijraset.com

Table1.1: Conformers and their Relative Gibbs free energies, Boltzmann populations of conformers of Ethyl (S)-(−)-4-chloro-3-hydroxybutyrate

Conformer	Relative ΔG (kcal/mol)	Population (%)
C_1	0.0	82.79
C_2	1.281	09.67
C_3	1.427	07.54

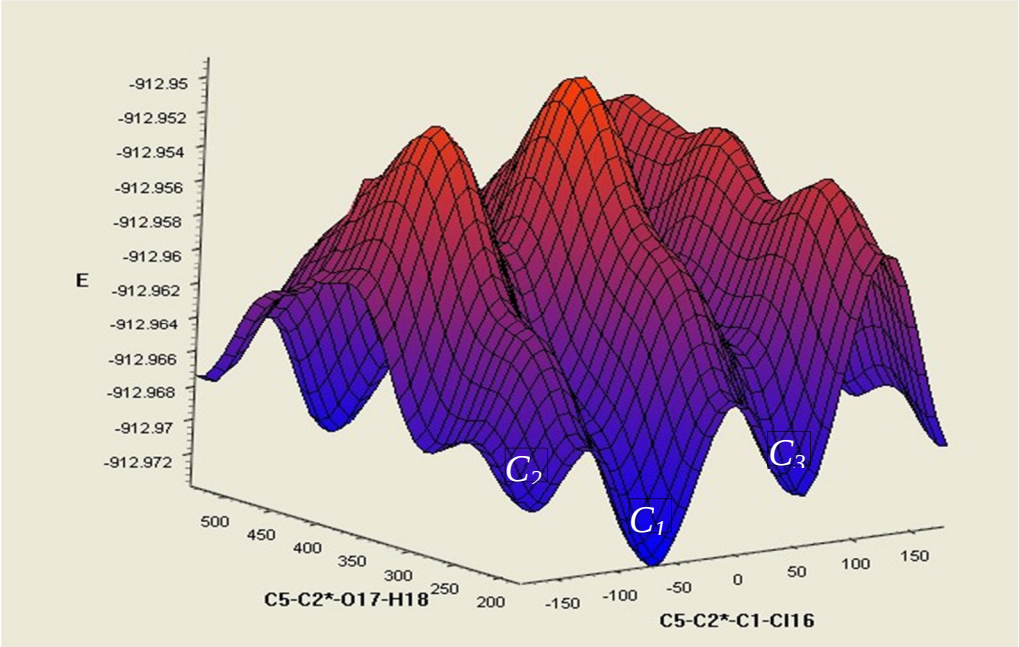

Fig. 1.3: PES scan curves for dihedral angles C5-C2*-C1-Cl16 and C5-C2*-O17-H18 yielding the most stable conformers C_1, C_2 and C_3.

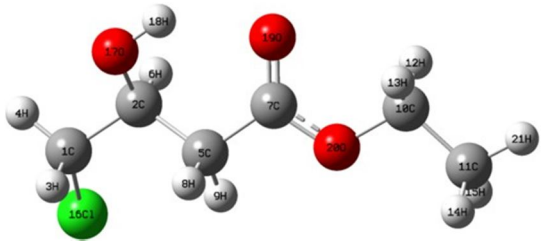

(a): C5-C2-C1-Cl16= -66˚, C5-C2-O17-H18= 57˚

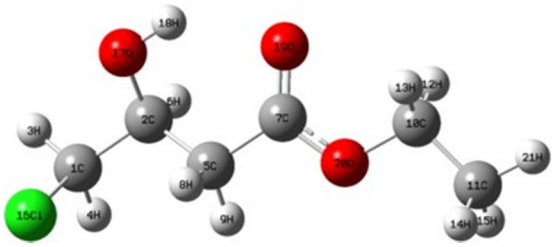

(b): C5-C2-C1-Cl16=55˚, C5-C2-O17-H18=55˚

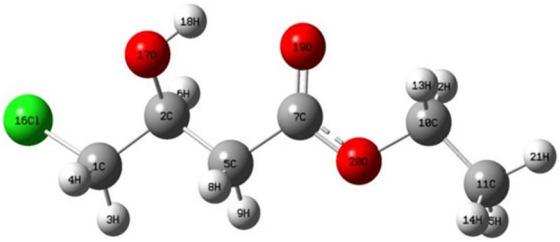

(c): C5-C2-C1-Cl16= -168˚, C5-C2-O17-H18=63˚

Fig.1.4: Conformers of Ethyl (S)-(−)-4-chloro-3-hydroxybutyrate at B3LYP/6-311+G(d,p)) level.

Table 1.2: Optimized geometrical parameters of the conformers C_1, C_2, C_3.

Parameters	Conformers		
Bond Length ($^{\circ}$)	**C_1**	**C_2**	**C_3**
C1-C2	1.525	1.523	1.522
C2-C5	1.533	1.537	1.540
C5-C7	1.512	1.513	1.516
C10-C11	1.513	1.515	1.515
C7-O20	1.222	1.222	1.341
C10-O20	1.455	1.455	1.455
C2-H6	1.098	1.105	1.100
C1-H3/H4	1.089	1.090	1.091
C5-H8/H9	1.096	1.096	1.098
C10-H12/H13	1.091	1.093	1.093
C11-H14/H15/H21	1.092	1.094	1.094
C2-O17	1.422	1.415	1.417
O17-H18	0.968	0.972	0.970
C1-Cl16	1.814	1.817	1.811
C7-O19	1.214	1.222	1.220
Bond Angle (deg)			
C2-C1-Cl16	112.0	114.1	112.4
C1-C2-C5/C2-C5-C7	112.8	112.3	112.2
C5-C7-O20	111.9	112.0	111.6
C7-O20-C10	116.9	116.8	116.8
C11-C10-O20	107.5	107.4	107.5
H4-C1-H3	109.6	109.8	109.9
C2-C1-H3	111.3	109.2	110.9
C2-C1-H4	109.6	110.6	110.1
C1-C2-H6	108.5	104.6	108.8
C5-C7-O19	124.6	124.6	124.8
O20-C7-O19	123.2	123.2	123.4
C2-O17-H18	106.4	106.7	106.7
Dihedral Angle (deg)			
C5-C2-C1-Cl16	-66.09	55.85	-168.3
C5-C2-O17-H18	57.18	54.40	63.02

Table 1.3: Relative Gibbs free energy and Boltzmann populations of four dimer species.

Dimer	Monomer Pair	Relative ΔG (kcal/mol)	Population (%)
D_1	C_1 with C_1	0.00	90.67
D_2	C_1 with C_2	1.703	5.21
D_3	C_1 with C_3	1.889	3.81
D_4	C_2 with C_2	3.401	0.31

In the next step we computed four dimer structures as -O-H•••O=C hydrogen bonded dimers from the three monomers. The four dimers D_i (i=1,2,3,4) with relative Gibbs free energies and populations are presented in Table 7.3. The most stable dimer D_1 is the most populated at ~91%. It is noted that the dimers D_2 and D_3 thinly populated while D_4 is negligible. In Fig. 7.5 we show the most stable *intra*-molecular monomer in comparison with the most stable *inter*-molecular dimer labelled with respective H•••O distances. The *intra* and *inter*-molecular hydrogen bonding parameters are given in Table 1.4.

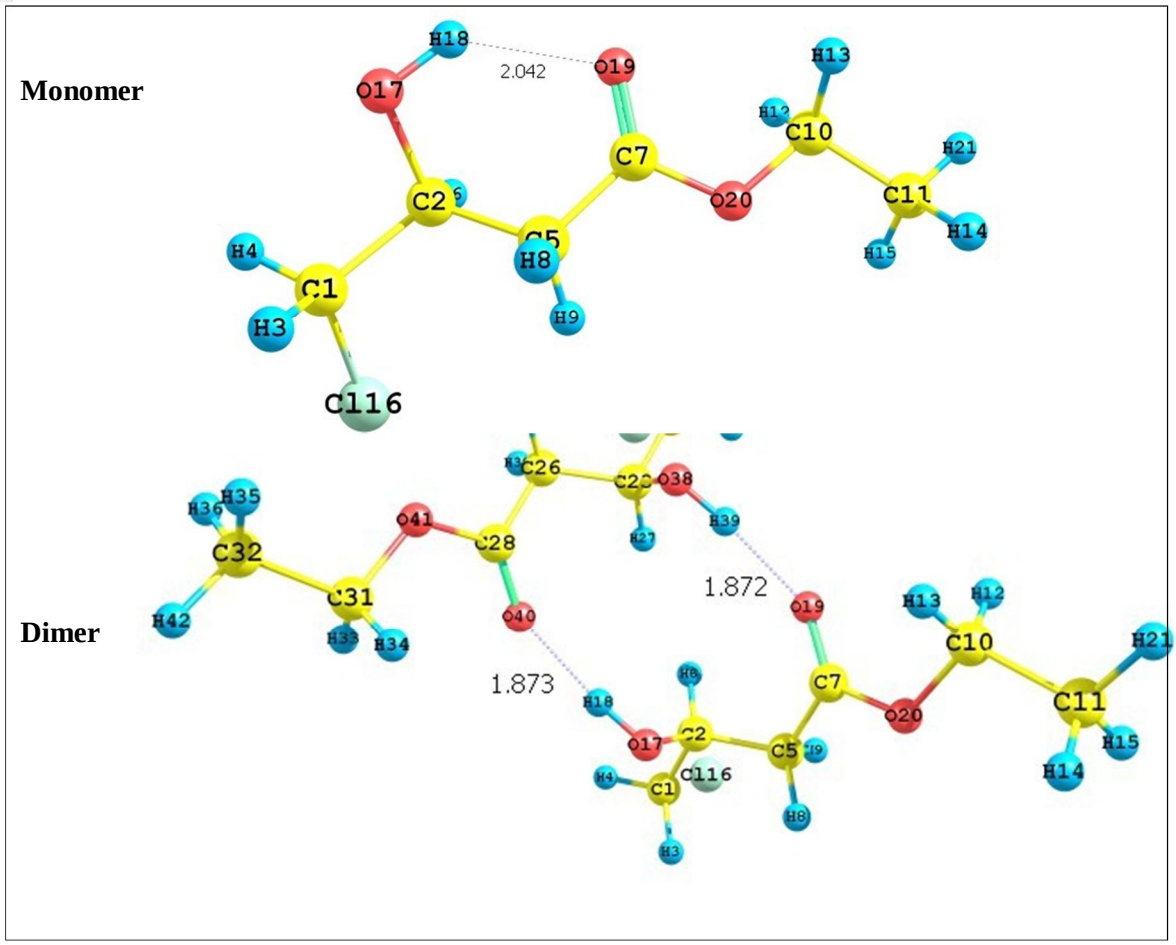

Fig. 1.5: Computed monomer and *inter*-molecular hydrogen bonded dimer with geometrical parameters of Ethyl (S)-(–)-4-chloro-3-hydroxybutyrate.

Table 1.4: Computed intra- and inter-molecular hydrogen bonding geometrical parameters of Ethyl (S)-(−)-4-chloro-3-hydroxybutyrate.

X-H•••Y	X-H (Å)	H•••Y (Å)	X•••Y (Å)	∠X-H•••Y (Deg)
Intra-molecular O−H•••O=C monomer	0.973	2.042	3.015	134
Inter-molecular O−H•••O=C dimer	0.973	1.872	2.845	173
**Standard Values*	0.969	2.724	3.694	-

In comparison we may say that the *inter*-molecular hydrogen bonded dimer agree better with the hydrogen bonding criteria, but we cannot rule out the possibility of *intra*- molecular monomer as well because the frequency correlation of monomer is also agreement with the observed which we will show in the next Section 1.2.2. This dilemma could be answered in some rigorous concentration dependent solution-phase IR spectral measurements. However, it has not been possible to ascertain by dimer calculations only as to which type of bonding is the determinant factor for the observed spectral features. Thus for tentative assignments we consider both *intra*- and *inter*-molecular hydrogen bonding. In nature *intra*-molecular hydrogen bonds are strong in comparison to *inter*-molecular hydrogen bonds. The H•••O bond distances in both types fall under the strong hydrogen bonding criteria but it is the *inter*-molecular type that is more favoured. The shift in the O-H and C=O frequency is only ~4% and 2% respectively, which contradicts the strength of the strong hydrogen bonding. Thus we characterize this as weak *inter*- molecular hydrogen bonding in Ethyl (S)-(−)-4-chloro-3-hydroxybutyrate.

2) *Vibrational Analysis:* Observed IR and Raman spectrum of Ethyl (S)-(–)-4-chloro-3-hydroxybutyrate are presented in Fig. 1.2. For a good agreement between experimental and theoretical spectra, we have plotted Boltzmann population-weighted IR spectra of monomers and dimers and are presented in Fig. 1.6 with experimental IR spectrum; likewise, the Fig. 1.7 give the Raman spectra, with lorentzian band width 4 cm^{-1}. A complete assignment of all the observed bands with that of monomer and dimer are presented in Table 1.5.

The O-H stretching band computed near 3577 cm^{-1} for a monomer in Fig. 1.6(c) shift to 3550 and 3541 cm^{-1} for the dimers in Fig.1.6(b) agreeing with the observed bands at 3452 cm^{-1} in Fig. 1.6(a). The carbonyl bands for intra-molecular monomer and inter-molecular dimer are computed at 1692 cm^{-1}. The observed band is at 1729 cm^{-1}, it being the strongest band in the spectrum. The Raman counterpart is a medium weak band at 1727 cm^{-1}. Another band is observed in IR at 1630 cm^{-1}. This is a weak shoulder to the earlier mode. These bands are assigned as C=O asymmetric and symmetric stretch. The dimer's bonded carbonyl band in Raman at 1692 cm^{-1} in Fig 1.7(b) is correlated to the observed band at 1727 cm^{-1} in Fig.1.7(a) and is assigned to the asymmetric carbonyl mode. The bands do not appear complimentary to each other, like we have already explained in the previous section about their lack of centre of inversion because the bands are not mutually exclusive. In Ethyl (S)-(–)-4-chloro-3-hydroxybutyrate, there are two pairs of –O-H and –C=O groups, with both participating in the hydrogen bonding. Both the pairs give rise to bands with frequencies too close to be resolved in the dimer spectrum. For example, two computed bands at 1692 and 1690 cm^{-1} are merged into a single band, and we may conclude that the contribution from both the pairs is equal.

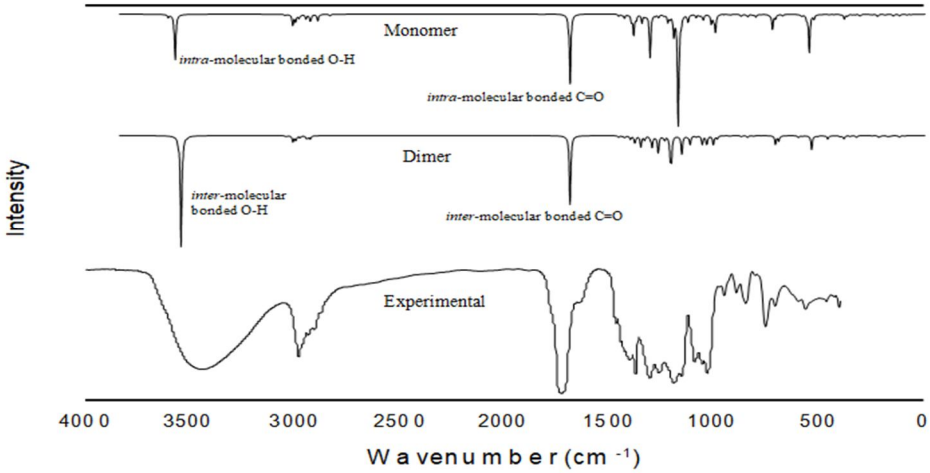

Fig. 1.6: Experimental, simulated dimer and monomer IR spectrum of Ethyl (S)-(−)-4-chloro-3-hydroxybutyrate.

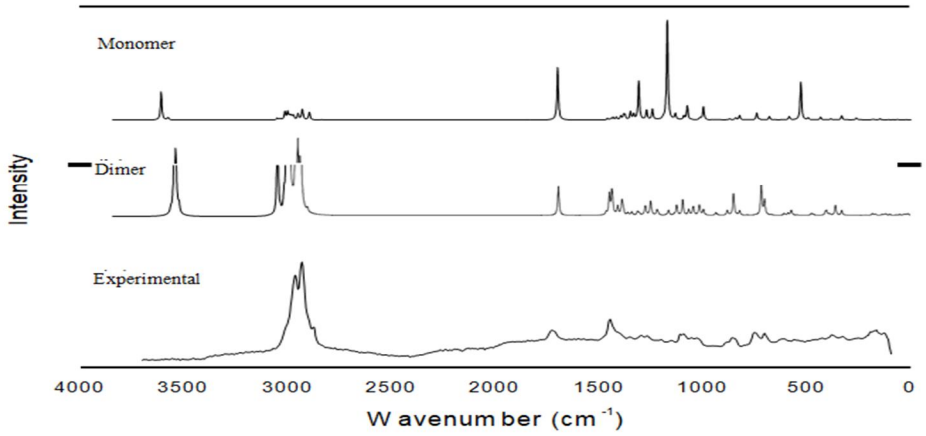

Fig. 1.7: Experimental (a), simulated dimer (b) and simulated monomer (c) Raman spectrum of Ethyl (S)-(−)-4-chloro-3-hydroxybutyrate (ordinate in Dimer spectrum is broken to adjust bands near 3500-3000 cm^{-1} from overshooting because of their large intensity.

Table 1.5: Vibrational frequencies of Monomer and Dimer with experimental IR and Raman frequencies and assignments of Ethyl (S)-(−)-4-chloro-3-hydroxybutyrate.

Computed Frequencies		Observed Frequencies		Assignments
Intra-molecular Monomer	Inter-molecular Dimer	IR	Raman	
3577	3550	-	-	O-H asym stretch
-	3541	3452 br ms	-	O-H sym stretch
3053	3049	-	-	CH_2 asym stretch (CH_2Cl)
3016	3016	-	-	CH_2 asym stretch (methyl-CH_2)
3003	3003	-	-	CH_2 asym stretch (methyl)
2999	2999	-	-	CH_2 asym stretch
2993	2993	-	-	CH_2 asym stretch (out of phase)
2987	2983	2982 m	2964 s	CH_2 sym stretch
2953	2953	-	-	CH_2 sym stretch (in phase)
-	2945	-	-	CH stretch
2933	2943	2929 m	2929 vs	CH_2-CH (CHOH) stretch
2897	2933	2910 m	2878 m, sh	Methyl sym stretch
1693	1692	1729 vs	1727 mw	C=O asym stretch
-	1690	1630 vw sh	-	C=O sym stretch
1461	1461	1466 sh	-	CH_2 scissoring
1445	1445	1445 v, sh	1449 mw	CH_2 scissoring (methyl)
1434	1434	1434 m sh	-	CH_2 asym deformation (methyl)
-	1430	1420 m, sh	-	CH_2 scissoring (CH_2Cl)
1400	1405	1401 m	1403 sh	CH_2 scissoring
1390	1386	1375 ms	-	O-H in plane bend
1377	1379	-	1360 w	CH_3 sym deformation (methyl, butterfly)
1350	1355	-	-	CH_2 wag
1336	1337	-	-	CH out of plane wag
1311	1310	1305 ms	1299 w	CH out of plane wag, O-H bend
1270	1274	1261 m	1271 w	O-H in plane bend
1245	1247	-	-	CH_2 twist (methyl, CH_2)
1226	1216	-	-	CH out of plane wag
1198	1210	1191 s	1205 w	CH out of plane wag
1177	1161	1152 m	1156 w	CHOH deformation
1132	1132	-	-	CH_2 rock (CH_2Cl-CH_2)
1130	1122	-	1112 w	CH_2 twist (CH_2Cl)
1091	1092	1093 m	1093 w	Methyl rock
1057	1062	1061 m	1059 w	C-C-C stretch (CH_2Cl-CHOH-CH_2)
-	1044	1031 m	1031 w	C-O stretch (CHOH)
1019	1013	-	-	C-O stretch (skeletal C-O)
999	993	949 vw	-	Skeletal C-C-C asym stretch
927	932	899 w	892 w sh	C-C stretch (CH_2-C=O)
877	877	863 w sh	862 w	CH_2 rock (near C=O)
845	848	848 w	850 w	Skeletal C-C-O deformation

806	818	-	-	CH_2 rock
780	783	756 w	754 mw	C-Cl stretch
727	714	710 w	707 mw	CH_2 twist (methyl)
-	699	-	-	C=O in plane wag
-	604	-	622 w	O-H out of plane deformation
587	586	598 w	-	O-H out of plane deformation
-	570	566 w	565 w	O-H out of plane deformation
552	541	-	-	O-H out of plane deformation
-	473	466 w	-	Skeletal deformation
458	464	-	-	Skeletal deformation
-	407	-	-	CHOH rock
401	400	405 w	-	CHOH rock
384	385	-	383 w	Skeletal C-C torsion
370	358	-	-	C-C-O deformation
251	252	-	258 w	Methyl torsion
226	221	-	-	C=O, O-H rock
191	180	-	-	Skeletal deformation
151	166	-	169 w	Skeletal deformation
121	122	-	127 w	Skeletal deformation

Note: Computed Frequencies (in cm^{-1}) are scaled with the factor 0.9613 [Scott, 1996] and Boltzmann population weighted, br=broad, sh=shoulder, s=strong, vs=very strong, ms=medium strong, w=weak, vw=very weak, mw=medium weak, sym=symmetric, asym=asymmetric.

The in-plane O-H deformation mode is a medium strong mode observed at 1375 cm^{-1}. The DFT computed values in both intra- and inter-molecular bonding are fairly computed. Characteristically it would have been a test to decide the type of hydrogen bonding involved if the DFT value in either bondings is correlated. The out of plane deformation modes are also weak but can be identified at 598 and 566 cm^{-1}, again the shift in the bands is negligible from where they are expected in the absence of hydrogen bonding. These modes due to CH, CH_2 and CH_3 have remained uninfluenced by the hydrogen bonding and are fairly accurately computed. The region 3000 - 2800 cm^{-1} is marked by a series of CH, CH_2 and CH_3 stretching modes [Belaidi, 2015; Guo, 2010].

Predicted bands agree very well with these modes though not all are observed. A very strong Raman mode at 2964 cm^{-1} and medium mode in IR at 2982 cm^{-1}, is assigned to CH_2 symmetric stretching and is also computed at the 2983 cm^{-1}. The CH_2-CH stretch mode is observed at 2929 cm^{-1} as medium IR and very strong Raman band. The methyl symmetric stretch mode is observed at 2910 cm^{-1} in IR and 2878 cm^{-1} in Raman. The region 1500 – 1100 cm^{-1} shows several deformation modes arising from CH, CH_2 and CH_3 groups. The medium band 1449 cm^{-1} (Raman) is correlated to 1445 cm^{-1} (DFT) mode and is assigned as CH_2 scissoring mode. Another medium strong mode at 1434 cm^{-1} (IR) is due to CH_2 deformation coming from the methyl group. At 1360 cm^{-1} (Raman) is the CH_3 symmetric deformation. It is computed at 1379 cm^{-1}. Vibrations of skeletal stretching and deformation modes have appeared in 1100-850 cm^{-1} region. A medium IR band at 1061 cm^{-1} is a mode due to C-C-C stretching. Another weak IR mode is identified as the C-C-C asymmetric stretch. Two modes are further computed and assigned to C-O at 1031 cm^{-1} in both IR and Raman, and 1013 cm^{-1} DFT computed. The skeletal C-C-O deformation mode is identified at 899 cm^{-1}. The skeletal and COOH deformation are weak in IR and Raman and observed at 848 cm^{-1}.

We may say that though the O-H•••O modes are localized in the dimer structure, the vibrational structure in IR spectrum is considerably modified with visible features near 3550-3400 cm^{-1} and 1730 cm^{-1}.

3) *IR And DFT-VCD Correlation:* Fig. 1.8 shows Boltzmann weighted-VCD spectrum for monomer and dimer, correlated with observed IR spectrum for the region 2000−400 cm^{-1} and the assignments are given in Table 1.6. The region is highly marked by the bands due to linear and oscillatory vibrations. From Fig.1.8 we can identify that the weak or shoulder bands in IR correspond to positive or negative bands. The assignments are as follows (Table 1.6).

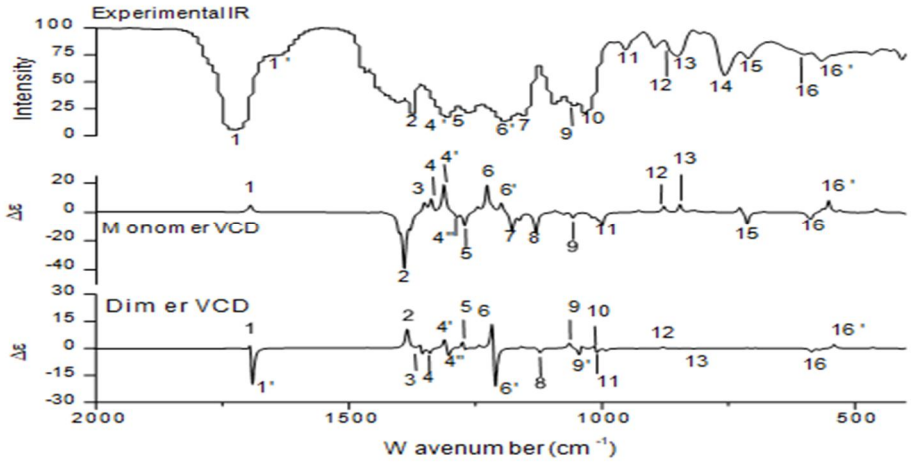

Fig. 1.8: Experimental IR, Simulated Monomer and dimer VCD spectrum of Ethyl (S)-(−)-4-chloro-3-hydroxybutyrate

The 1729 cm^{-1} broad band in IR is split into two bisignate VCD dimer bands as **1**, **1''**. They are assigned to the C=O stretch asymmetric and symmetric stretch in the dimer. The intra-molecular monomer VCD has produced only band at 1693 cm^{-1}. It is assigned as **1**, because of the free C=O stretch in the unbound state. The band **2** is the O-H in plane bend coupled with CH wag, while band **3** is exclusively CH wag. Bands **4** and **4'** belong to the CH wag mode; the latter being a coupled mode with O-H bend. The band **5** is exclusively O-H in plane bend. Bands **6** and **6'** belong to CH wag of different CH groups while **7**, **8** are individually contributing. Two bands **9** and **9'** are the C-C-C stretch modes in the dimer VCD.

Table 1.6: Correlation of experimental IR frequencies with simulated Monomer and Dimer VCD bands

Band No.	Intra-molecular Monomer	Inter-molecular Dimer	IR	Assignments
1	1693	1695	1729	C=O asymmetric stretch
1'	-	1687	1630	C=O symmetric stretch
2	1390	1383	1375	O-H in plane bend, CH wag
3	1350	1354	-	CH_2 wag
4	1336	1335	-	CH out of plane wag
4'	1311	1310	1305	CH out of plane wag, O-H bend
4''	1282	1297	-	CH out of plane wag,
5	1270	1274	1261	O-H in plane bend
6	1226	1216	-	CH out of plane wag
6'	1198	1210	1191	CH out of plane wag
7	1177	-	1152	CHOH deformation
8	1130	1122	-	CH_2 twist (CH_2Cl)
9	1057	1062	1061	C-C-C stretch
9'	-	1044	-	C-C-C stretch
10	-	1013	1031	C-O stretch (skeletal C-O)
11	999	1005	949	Skeletal C-C-C asymmetric stretch
12	877	-	863	CH_2 rock (near C=O)
13	845	-	848	Skeletal C-C-O deformation
14	780	783	756	C-Cl stretch
15	712	-	710	CH_2 twist (methyl)
16	587	586	598	O-H out of plane deformation
16'	552	541	566	O-H out of plane deformation

The band 14 is the C-Cl stretch band. It is a weak band in IR while we have not been able to identify the same in VCD because the rotational strength is very small. The bands 16 and 16' are the O-H out of plane bending vibration. We see that certain bands in VCD are not identified like bands 1 and 10 in monomer and 7, 12, 13 and 15 in dimer. These bands have been computed but the magnitudes of their corresponding rotational strengths are very small and hence they are difficult to place in the VCD spectra.

II. CONCLUSIONS

The DFT intra-molecular monomer and inter-molecular-dimer model proposed with O-H•••O=C type of hydrogen bonding has been satisfactory in accounting for the experimental IR and Raman spectral band features of Ethyl (S)-(–)-4-chloro-3- hydroxybutrate. Three stable monomers have shown the possibility of four dimer structures, with varying Boltzmann populations. The most stable monomer also forms the most stable dimer with ~90% population. It could be said that both *intra*- and *inter*- molecular hydrogen bondings may exist in the sample.

To resolve this further rigorous concentration-dependent solvent experiments and study, or near IR spectrum could be attempted based on the fact that *inter*-molecular hydrogen bonds are broken by dilution with non-polar solvents, whereas *intra*-molecular bonds are independent of the concentration; which is the future plan of work. The computed geometrical parameters for the hydrogen bond lengths are reasonably accurate and are in favor of O-H•••O=C type of hydrogen bonding but the shift in the bonded frequencies conclude the bonding as weak *inter*-molecular hydrogen bonding.

III. ACKNOWLEDGMENT

The authors wish to gratefully to acknowledge Prof C.K Dixit, Dean Department of Physics, D.S.M.N.R U , Lucknow.

REFERENCE

[1] [Zhou, 1983; Karanewsky, 1990]
[2] [Aragozzini, 1992; Patel, 1992; Shimizu, 1990]
[3] www.sigmaaldrich.com
[4] M. Suzuki, T. Shimanouchi, J. Mol. Spectro. 28 (1968) 394-410
[5] M. Suzuki, T. Shimanouchi, J. Mol. Spectro. 29 (1969) 415-425.M.J. Frisch, G.W. Trucks,
[6] H.B. Schlegel, G.E. Scuseria, M.A. Robb, J.R. Cheeseman, G.Scalmani, V. Barone, B. Mennucci,
[7] G.A. Petersson, H. Nakatsuji, M. Caricato, X. Li, H.P.Hratchian, A.F. Izmaylov, J. Bloino, G. Zheng,
[8] J.L. Sonnenberg, M. Hada, M. Ehara, K. Toyota, R.34 Fukuda, J. Hasegawa, M. Ishida, T. Nakajima,
[9] Y. Honda, O. Kitao, H. Nakai, T. Vreven Jr, J.A. Montgomery, 1 J.E. Peralta, F. Ogliaro, M. Bearpark,
[10] J.J. Heyd, E. Brothers, K.N. Kudin, V.N. Staroverov, R. Kobayashi, J. Normand, K. Raghavachari,
[11] A. Rendell, J.C. Burant, S.S. Iyengar, J.Tomasi, M. Cossi, N. Rega, J.M. Millam, M. Klene,
[12] J.E. Knox, J.B. Cross, V. Bakken, C. Adamo, J. Jaramillo, R. Gomperts, R.E. Stratmann, O. Yazyev,
[13] A.J. Austin, R. Cammi, C. Pomelli, J.W. Ochterski, R.L. Martin, K. Morokuma, V.G. Zakrzewski,
[14] G.A. Voth, P. Salvador, J.J. Dannenberg, S. Dapprich, A.D. Daniels, Ö. Farkas, J.B. Foresman, J.V.
[15] Ortiz, J. Cioslowski, D.J. Fox, Gaussian 09, Revision A.1 Gaussian, Inc., Wallingford CT, 2009.

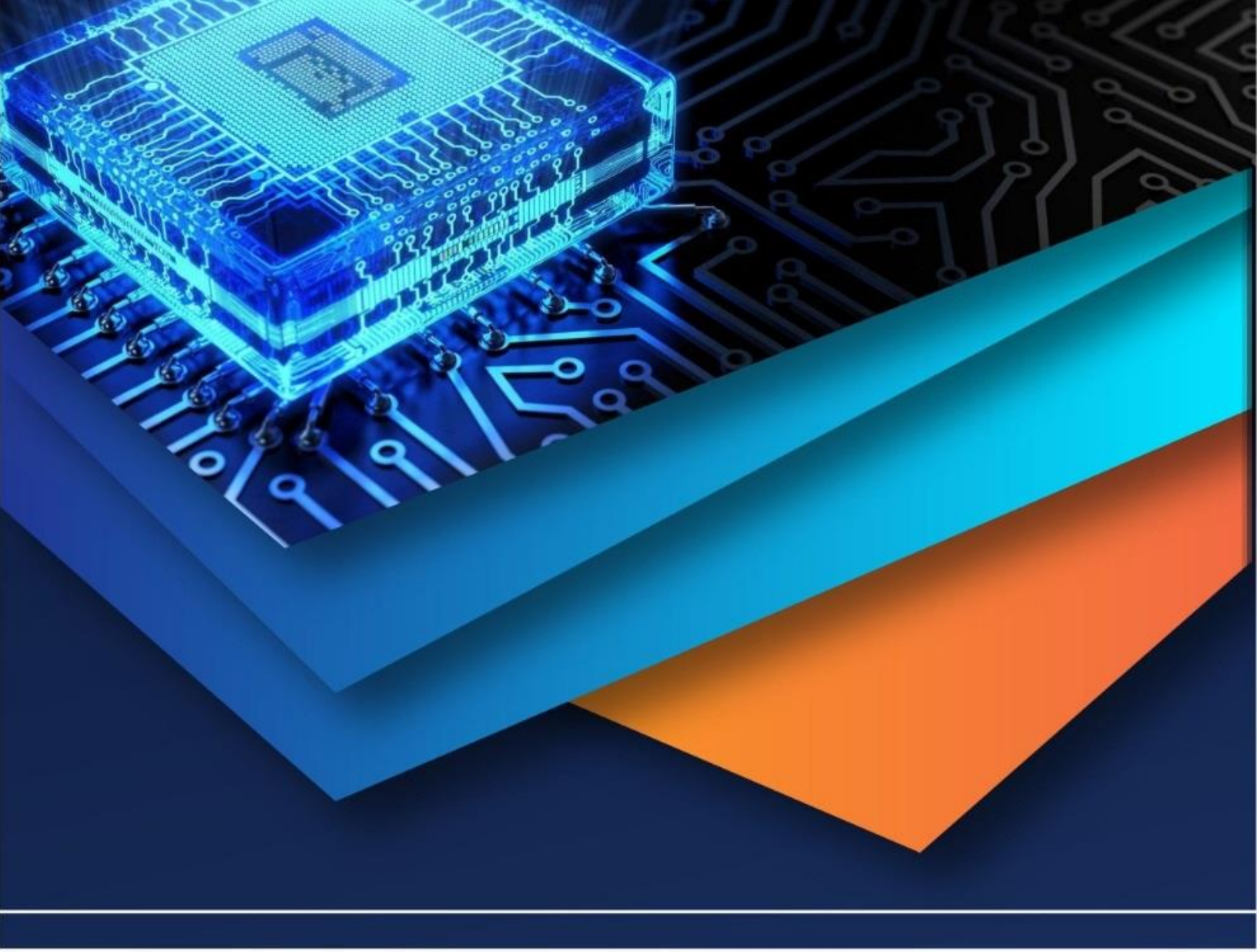

10.22214/IJRASET

45.98

IMPACT FACTOR: 7.129

IMPACT FACTOR: 7.429

INTERNATIONAL JOURNAL FOR RESEARCH

IN APPLIED SCIENCE & ENGINEERING TECHNOLOGY